Journal Name

ARTICLE

Received 00th January 20xx,

Accepted 00th January 20xx

DOI: 10.1039/x0xx00000x

www.rsc.org/

Genesis of Bi-functional Acid-Base Site on Cr-supported Layered Double Hydroxide Catalyst Surface for One-pot Synthesis of Furfurals from Xylose with Solid Acid Catalyst

M. Shirotori,[a] S. Nishimura,[a,b] and K. Ebitani[a,b]

Cr-supported Mg-Al layered double hydroxide (Cr/Mg-Al LDH) composed bi-functional Lewis acid – Brønsted base active sites on the catalyst surface at close boundaries between Cr^{3+} oxide and Mg-Al LDH. These proceeded to efficient aldose–ketose isomerization. The combined use of solid Brønsted acid Amberlyst-15 and bi-functional acid–base Cr/Mg-Al LDH exhibits higher activity for one-pot transformation of xylose into furfural *via* aldose–ketose isomerization and successive dehydration under mild conditions than the activity shown by basic bare Mg-Al LDH, substituted Mg-Cr LDH, and Lewis acidic Cr^{3+} supported catalysts with Amberlyst-15. Correlation between the activity and the Cr loading amount for Mg-Al LDH was evaluated using several characterizations and MPV reduction as a model reaction for Lewis acidity investigation. Results show the following: (1) The monomer of Lewis acidic Cr^{3+} oxide is supported on the Mg-Al LDH surface below 1 wt%. (2) Thereafter, Cr^{3+} species form Lewis acidic small Cr^{3+} oxide dimer and/or trimer up to 5 wt%. Then they cover the Mg-Al LDH surface to generate highly active bi-functional Lewis acid – Brønsted base sites. (3) Above 5 wt%, the excess Cr^{3+} species generate inert Mg-Cr and/or Mg-Al-Cr LDH like composites. These deposit on some active sites, leading to decreased activity. Results show that the furfural yields vary significantly in accordance with Cr loadings, and the 5wt%Cr/Mg-Al LDH achieves the highest value (59% yield, 18 h) because the most effective interaction between the Lewis acidic Cr^{3+} oxide and Mg-Al LDH basic site is produced at 5 wt% Cr loading.

Introduction

A well-known layered clay mineral, Mg-Al layered double hydroxide (Mg-Al LDH; $[Mg_{1-x}^{2+}Al_x^{3+}(OH)_2]^{x+}A_{x/n}^{n-}\cdot mH_2O$), possesses Brønsted base sites as adsorbed carbonate and hydroxide ions at its surface of brucite-like positive charged two-dimensional sheets. LDH has been widely used as solid base catalyst and support for metal catalysts such as Ru, Pd, Ag, Au, and Pt.[1-7] As a Brønsted base solid catalyst, LDH shows catalytic activity for various organic reactions such as Knoevenagel condensation,[8-11] epoxidation,[12-13] transesterification,[14] and aldol condensation[15-16] as well as aldose–ketose isomerization.[11, 17-19]

Conversion of biomass resources into value-added chemicals and fuels has attracted much attention because such materials can serve as sustainable non-petroleum building blocks in biorefineries.[20-23] Lignocellulosic biomass, a renewable carbon source composed mainly of cellulose, hemicellulose, and lignin, is known as the most abundant woody biomass.[24-26] The hydrolysis of cellulose and hemicellulose into monosaccharides such as glucose and xylose, the first step in biorefinery operations, has been demonstrated with enzyme and chemical catalysts such as soluble mineral acids and solid acids,[27-28] acidic carbons,[29-32] sulfonated carbons,[33-35] and biomass-derived carbon-based catalyst.[36]

The successive conversion of glucose and xylose into furans such as 5-(hydroxymethyl)furfural and furfural has been emphasized because they have great potential as non-petroleum substrates in production of polymers, pharmaceuticals, biofuels, and fine chemicals.[19, 25-26, 37-38] Because this reaction proceeds trimolecular dehydration, Brønsted acid catalysts such as sulfonated zirconia,[39] porous niobium silicates,[40] sulfonic acid modified mesoporous shell silica beads,[41] arenesulfonic SBA-15,[42] and zeolite-based catalysts[43-46] have conventionally been applied at high reaction temperatures (>423 K).

As advanced research studies, many researchers have recently reported two-step transformations of monosaccharides into furans *via* aldose–ketose isomerization and dehydration of ketose. A benefit of this two-step reaction path is that it reduces the energy used for dehydration. For example, the reported activation barrier of xylose (aldopentose) is approximately 30–32 kcal/mol,[47-48] whereas that of xylulose (ketopentose) was calculated as 23.1 kcal/mol.[49] In fact, in this two-step reaction system, the reaction temperature can be reduced to 373 K with 29–56% yield of furfural.[18, 50-51] However, because aldose–ketose isomerization is an

[a] School of Materials Science, Japan Advanced Institute of Science and Technology, 1-1 Asahidai, Ishikawa, Nomi, 923-1292, Japan.
[b] Graduate School of Advanced Science and Technology, Japan Advanced Institute of Science and Technology.

† Footnotes relating to the title and/or authors should appear here.
Electronic Supplementary Information (ESI) available: [details of any supplementary information available should be included here]. See DOI: 10.1039/x0xx00000x

equilibrium rate-determining reaction and because the subsequent dehydration of ketopentose is a one-way reaction in a two-step system, discovery of a highly active catalyst surface in aldose–ketose isomerization has been the crucial factor for additional activation. Both Lewis acid sites and base sites are active, respectively, for aldose–ketose isomerization *via* hydride shift and proton shift reaction.[52] Binder *et al.*[50] and Suzuki *et al.*[51] have respectively demonstrated two-step dehydration of xylose into furfural composed of isomerization over Lewis acid site and successive dehydration over Brønsted acid site under mild conditions (373 K) using $CrCl_2$ with LiBr and SO_4^{2-}/SnO_2.

Our earlier studies have demonstrated that furfural can be formed effectively from xylose in a one-pot manner involving aldose–ketose isomerization over Mg-Al LDH *via* proton shift of pentose and successive dehydration of xylulose into furfural over Brønsted acid Amberlyst-15 at 373 K.[18] This catalytic system also shows activity to direct synthesis of furfural derivatives such as (2-furanylmethylene)malononitrile (FMM), known as a semiconducting organic material for photovoltaic device fabrication,[53] from xylose in a one-pot manner *via* successive Knoevenagel condensation by base site of Mg-Al LDH. As advanced research studies, we have reported that the Cr-supported Mg-Al LDH catalyst (Cr/Mg-Al LDH), which is composed of Mg-Al LDH carrier and immobilized Cr^{3+} oxide onto LDH surface, showed higher activity to aldose–ketose isomerization as a bi-functional Lewis acid – Brønsted base catalyst than bare Mg-Al LDH.[11] Furthermore, we have demonstrated a similar strategy in the presence of a different family of bi-functional Lewis acid – Brønsted base Ni^{2+}-modified Al_2O_3 catalyst.[54] The bi-functional Lewis acid – Brønsted base site might act as a highly effective active site for aldose–ketose isomerization. Nevertheless, the detailed local structure of the bi-functional site, the optimized surface structure, and the method for preparing the optimum bi-functional Lewis acid – Brønsted base catalyst for aldose–ketose isomerization remain open questions.

This report describes the genesis of a bi-functional Lewis acid – Brønsted base site on Cr/Mg-Al LDH for one-pot transformation of xylose into furfurals. This study was conducted to elucidate the origin of specific high activity for xylose isomerization over the bi-functional acid–base site. A detailed local structure of surface Cr cation species with various Cr loadings was proposed from physicochemical measurements taken using XPS, XAS, ESR, and DTA. We revealed the significance of a bi-functional Lewis acid – Brønsted base site on Cr/Mg-Al LDH generated at close boundaries between small clusters of Cr^{3+} oxide and LDH base sites by comparing catalytic activity with other Cr-supported catalysts and MPV reduction of furfural as a model reaction to evaluate Lewis acidity.

Experimental

Materials and synthesis of catalysts

Materials. Mg-Al LDH (AD500NS; Mg/Al = 3.1, MgO 38.1%, Al_2O_3 15.7%, CO_2 8.1%) was purchased from Tomita Pharmaceutical Co., Ltd. $CrCl_3{\cdot}6H_2O$, $MgCl_2{\cdot}6H_2O$, AlOOH (boehmite), CeO_2, and 2-propanol were supplied by Wako Pure Chemical Industries Ltd. *N*,*N*-dimethylformamide, xylose, and TiO_2 (rutile) were obtained from Kanto Chemical Co. Inc., whereas TiO_2 (anatase) and γ-Al_2O_3 (JRC-ALO-8) were supplied respectively by Tokyo Chemical Industry Co. Ltd. and the Catalysis Society of Japan. Amberlyst-15 was purchased from Sigma-Aldrich Corp. Furfural and malononitrile were obtained from Acros Organics BVBA.

Preparation of catalysts. Cr/Mg-Al LDHs were prepared using an impregnation method (adsorption) with Mg-Al LDH and an aqueous solution of $CrCl_3{\cdot}6H_2O$: $CrCl_3{\cdot}6H_2O$ was dissolved in 100 mL of distilled water. Then 2 g of Mg-Al LDH was added. After stirring at 353 K for 24 h, the obtained **greenish** paste was filtered and washed with 2 L of distilled water. Then it was dried overnight at 383 K.

Mg-Cr LDH (Mg/Cr = 3) was prepared by co-precipitation. An aqueous solution of $MgCl_2{\cdot}6H_2O$ and $CrCl_3{\cdot}6H_2O$ ($[M^{2+}] + [M^{3+}] = 1$ M, 40 mL) and an aqueous NaOH solution (1.0 M) were dropped slowly into an aqueous solution of Na_2CO_3 (1.5 M, 40 mL) with stirring at room temperature and pH 10.0. Then the resulting solution was stirred at 338 K for 6 h. The obtained paste was filtered, washed with 2 L of distilled water, and then dried at 383 K overnight.

Characterizations

X-ray diffraction (XRD). XRD patterns were collected on a SmartLab (Rigaku) using a Cu Kα X-ray source (40 kV, 30 mA).

Nitrogen adsorption. Nitrogen adsorption measurements were taken to ascertain the BET specific surface area. Measurements were taken at 77 K (BELSORP-max; BEL Japan, Inc.).

X-ray photoelectron spectroscopy (XPS). XPS analyses were performed (Kratos AXIS-URTRA DLD; Shimadzu Corp.) using a monochromatic Al Kα source (10 mA, 15 kV). The binding energies were calibrated with C 1s level (284.5 eV) as the internal standard.

X-ray absorption spectra (XAS). XAS in Cr K-edge were recorded at room temperature using double Si(111) single-crystal monochromator at the BL-9C station of KEK-PF, Japan (Proposal No. 2013G586). The obtained spectra were analyzed using software (ver. 2.5.92REX2000; Rigaku Corp.).

Electron spin resonance (ESR). Solid state electron spin resonance (ESR) spectra were produced (JES-FA200; JEOL) at X-band frequency with a 100 kHz modulation frequency, 1 mW microwave power, and 0.6 mT modulation width. Spectra were recorded at 103 K.

Differential thermal analysis (DTA). DTA curves were corrected on a Thermo plus EVO2 (Rigaku Corp.) with a rewarming rate of 10°C min^{-1} in air.

Transmission electron microscopy (TEM). TEM images were taken (H-7100; Hitachi Co. Ltd.) at 100 kV.

Reactions

One-pot synthesis of furfural. One-pot synthesis of furfural from xylose was performed in a Schlenk tube attached to a reflex condenser under an N_2 flow (30 mL min^{-1}). The reaction was typically performed using 0.67 mmol of xylose, 0.2 g of Cr-LDHs or Mg-Al LDH, 0.1 g of Amberlyst-15 and 3 mL of *N*,*N*-dimethylformamide at 373 K.

One-pot synthesis of FMM. One-pot synthesis of FMM from xylose, which consists of furfural synthesis and successive Knoevenagel condensation was conducted *via* a two-step reaction without catalyst separation: after furfural synthesis, the reaction mixture was cooled to room temperature without stirring, then 0.8 mmol of malononitrile was added; thereafter, the following Knoevenagel

condensation was conducted under stirring at 373 K. The yields of furfural and FMM were calculated based on xylose.

Meerwein–Ponndorf–Verley (MPV) reduction. The MPV reduction of furfural in 2-propanol toward furfuryl alcohol was performed in 50 mL of a pear-shaped flask attached to a reflex condenser. After 1.3 mmol furfural, 83 mmol 2-propanol (6.4 mL), and 0.1 g of catalysts were charged into the reactor, they were heated at 355 K.

Products obtained from one-pot synthesis of furfural and FMM from xylose, and from MPV reduction were analyzed using GC-FID (GC-2014; Shimadzu Corp.) equipped with a non-polar column (DB-1; Agilent Technologies Inc.), whereas isomerization of xylose was analyzed using HPLC (515; Waters Corp.) with a column (RSPak KC-811; Shodex, Showa Denko K.K.). The HPLC analysis conditions were set as 0.1 wt% H_3PO_4 aq. eluent, 1.0 mL min^{-1} flow rate, and 323 K column temperature.

RESULTS AND DISCUSSION

Effects of Cr species location. Preliminarily, we prepared Cr-LDHs with different location of Cr species. Then we investigated their catalytic performance and structural properties. The substituted type Mg-Cr LDH had a typical LDH structure. The supported type 9wt%Cr/Mg-Al LDH retained the original Mg-Al LDH structure ascertained from XRD measurements (Figure 1(A)). This result indicates that, the Cr species are mainly supported on Mg-Al LDH surface as small clusters in the case of 9wt%Cr/Mg-Al LDH. The XPS analyses of Cr/Mg-Al LDH and Mg-Cr LDH revealed Cr $2p_{2/3}$ peaks at 576.5 eV and 577.0 eV, respectively corresponding to the Cr^{3+} oxide and hydroxide[55] (Figure 1(B)). X-ray absorption near-edge structure (XANES) features of both Cr-LDHs in Cr *K*-edge XAS were similar to those of Cr^{3+} compounds. Moreover, because strong pre-edge peaks at around 5992 eV attributed to tetrahedral Cr species were observed only slightly in prepared Cr-LDHs, the Cr species in those Cr-LDHs are expected to exist only as octahedral compounds (Figure 1(C)). From these results, the following structural properties of Cr-LDHs were inferred: The small octahedral cluster of Cr^{3+} oxide species is present on the Mg-Al LDH surface in the case of Cr/Mg-Al LDH, whereas $Cr(OH)_3$ constituted the LDH octahedral hydroxide layers with $Mg(OH)_2$ in the case of Mg-Cr LDH.

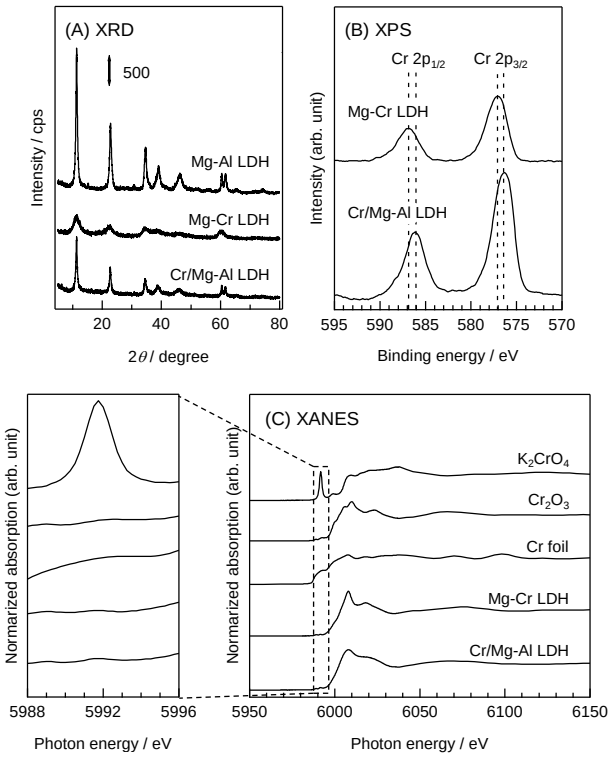

Figure 1. (A) XRD patterns, (B) Cr 2p XPS, and (c) Cr *K*-edge XANES of 9wt%Cr/Mg-Al LDH and Mg-Cr LDH (Mg/Cr = 3).

Table 1 presents the results of furfural yield in one-pot dehydration of xylose using the pair of Amberlyst-15 and supported type Cr/Mg-Al LDH, the substituted type Mg-Cr LDH, or the physical mixture of Mg-Al LDH and Cr_2O_3. The combined use of Amberlyst-15 and bare Mg-Al LDH, and blank test (just loading Amberlyst-15) were also tested. The table shows that just loading Amberlyst-15 was unsuitable for direct dehydration of xylose to furfural. The combined use of Amberlyst-15 and bare Mg-Al LDH gave 19% yield of furfural with ~30% selectivity and ~70% xylose conversion. The substituted type Mg-Cr LDH or the physical mixed type Mg-Al LDH + Cr_2O_3 system showed similar yield to that of bare Mg-Al LDH. Therefore, implementation of Cr^{3+} species or physical mixing of bulk Cr_2O_3 is unsuitable for xylose transformation. Higher performance was observed in the case of supported type Cr/Mg-Al LDH catalyst with 36% yield of furfural, ~40% selectivity of furfural, and ~85% xylose conversion. Isomerized pentoses selectivity was ~30%, and no other products were detected by GC-FID and HPLC. The combined use of Cr/Mg-Al LDH and Amberlyst-15 achieved 59% yield of furfural from xylose after optimization of Cr loading amount and reaction time (*vide infra*). These results demonstrate clearly that supporting the trivalent Cr species onto LDH surface is more effective than substitution or physical mixing.

Table 1. Activities of combined use of Cr-LDHs and Amberlyst-15 for one-pot synthesis of furfural from xylose[a]

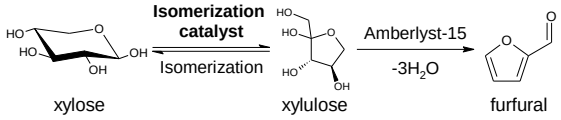

entry	isomerization catalyst	yield of furfural /%
1	Cr/Mg-Al LDH	36,[b] 59[c]
2	Mg-Cr LDH[d]	24
3	Mg-Al LDH + Cr_2O_3[e]	21
4	Mg-Al LDH	19
5	—	4

[a]Conditions: xylose (0.67 mmol), isomerization catalyst (0.2 g), Amberlyst-15 (0.1 g), *N*,*N*-dimethylformamide (3 mL), 373 K, 3 h, N_2 flow (30 mL min^{-1}). [b]Cr (9 wt%). [c]Cr (5 wt%), 18 h. [d]Mg/Cr = 3. [e]Mg-Al LDH (0.174 g) + Cr_2O_3 (0.026 g).

To investigate the effect of Cr^{3+} loading onto Mg-Al LDH on the activity for xylose isomerization, we examined the transformation of xylose over Cr/Mg-Al LDH and bare Mg-Al LDH in the absence of Amberlyst-15. The retention times for detected compounds were, respectively, 7.5, 7.7, and 8.0 min for xylose, xylulose and lyxose, for ribulose, and for arabinose (see Figure S1). The supported type Cr/Mg-Al LDH exhibited higher xylose conversion and isomerized pentose selectivity, as shown in the obtained HPLC charts (Figure S1) and exhibited rough calculated values (Table S1). These results suggest that the immobilization of Cr species on Mg-Al LDH surface

affected not only promotion of the reaction rate but also suppression of side reactions, such as oligomerization or decomposition.

Table 2 presents the Lewis acidity of various Cr-LDHs as its catalytic activity for the MPV reduction of furfural in 2-propanol toward furfuryl alcohol, a typical hydride shift reaction catalyzed by a Lewis acid such as γ-Al_2O_3 (entry 5).[11] It is noted that solid base catalysts, such as MgO and CaO, have also been reported affording high activity in the MPV reduction.[56-59] However, these typical solid base catalysts usually required a pretreatment with high temperature to generate the basic O^{2-} anion because these Lewis base sites are easily poisoned by CO_2 and H_2O in the atmosphere.[60] In fact, un-pretreated MgO showed no activity for the MPV reduction (entry 7). Accordingly, the catalytic performance for MPV reduction in this reaction conditions should be mainly influenced by the Lewis acidity. Our earlier study demonstrated that Cr/Mg-Al LDH exhibited higher activity to the MPV reduction than bare Mg-Al LDH, as shown in entries 1 and 2. Therefore, we compared the activities of supported type Cr/Mg-Al LDH with substituted type Mg-Cr LDH in the MPV reduction. As shown in entry 3, the activity of Mg-Cr LDH resembled that of bare Mg-Al LDH. It was much lower than Cr/Mg-Al LDH. These results suggest that supporting Cr^{3+} species onto the Mg-Al LDH surface is suitable to provide Lewis acidity rather than substituting Cr^{3+} species in Mg-Cr LDH. They also suggest that the Cr/Mg-Al LDH surface consisted of LDH-originated Brønsted base sites and supported Cr^{3+}-originated Lewis acid sites. Cr/Mg-Al LDH showed higher activity for furfural production from xylose than bare Mg-Al or Mg-Cr LDH surface, which is composed mainly of Brønsted base sites. Therefore, the Brønsted base – Lewis acid bi-functional Cr/Mg-Al LDH surface might function more efficiently for xylose conversion. Moreover, because this MPV reduction was only slightly promoted over the bulk Cr_2O_3 surface (entry 4), dispersion of Cr^{3+} species is expected to play an important role in generating Lewis acidity.

Table 2. Activities of Cr-LDHs for MPV reduction of furfural[a]

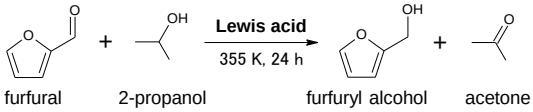

entry	catalyst	yield of furfuryl alcohol /%
1	Cr/Mg-Al LDH[b]	33
2	Mg-Al LDH	9
3	Mg-Cr LDH[c]	7
4	Cr_2O_3	trace
5	γ-Al_2O_3	74
6	Amberlyst-15	0
7	MgO	0

[a]Conditions: furfural (1.3 mmol), 2-propanol (83 mmol), catalyst (0.1 g), 355 K, 24 h. [b]Cr (9 wt%). [c]Mg/Cr = 3.

Effect of support. To evaluate the bi-functional Lewis acid – Brønsted base surface, various Cr^{3+} supported catalysts (Cr/Support) were prepared to assess its catalytic activities for MPV reduction and one-pot synthesis of furfural from xylose in the presence of Amberlyst-15. As Cr^{3+} supports, SiO_2, CeO_2, TiO_2(rutile), TiO_2(anatase), AlOOH, and γ-Al_2O_3 were selected in addition to Mg-Al LDH. The Cr content was adjusted to 9 wt%.

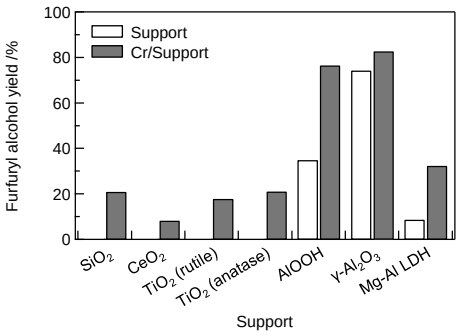

Figure 2. Activities of various supports and Cr/Support catalysts for MPV reduction. Conditions: furfural (1.3 mmol), 2-propanol (83 mmol), catalyst (0.1 g), 355 K, 24 h, amount of Cr (9 wt%).

All Cr^{3+} supported catalysts retained original their respective support structures determined using XRD (Figure S2). The XPS analysis results suggested that the oxidation states of Cr species on CeO_2, TiO_2(rutile), TiO_2(anatase), AlOOH, and γ-Al_2O_3 were Cr^{3+} oxides, and that of Cr/SiO_2 was Cr^{3+} hydroxide[55] (Figure S3). Lewis acidities evaluated as activity for the MPV reduction over bare supports and Cr supported catalysts are presented in Figure 2. The use of bare SiO_2, CeO_2, TiO_2(rutile), and TiO_2(anatase) gave furfuryl alcohol only slightly. Nevertheless, furfuryl alcohol production was observed over Cr supported SiO_2, CeO_2, TiO_2(rutile), and TiO_2(anatase). Therefore, we infer that the impregnation of Cr^{3+} onto these supports, which themselves possess no active Lewis acidic site for MPV reduction, causes generation of Lewis acidity. Furthermore, increasing Lewis acidity by Cr^{3+} support was observed for Lewis acidic AlOOH and γ-Al_2O_3 which showed medium or high activity for MPV reduction even support itself. These results show clearly that supported Cr^{3+} species can act as a Lewis acid site and can promote MPV reduction irrespective of the support.

Figure 3 presents the furfural yield from xylose by combined use of Amberlyst-15 and bare or Cr^{3+} supported catalysts. In the case of combined use of Amberlyst-15 and bare SiO_2, CeO_2, TiO_2(rutile), and TiO_2(anatase), which are inactive for MPV reduction, gave poor furfural yield. Furfural amounts obtained using those catalysts were similar to that of Amberlyst-15 alone (approx. 5%). Therefore, these

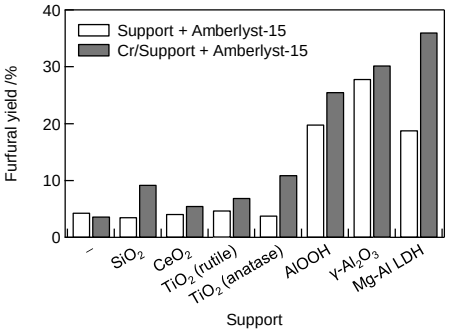

Figure 3. Activities of combined use of various supports or Cr/Supports as isomerization catalysts and Amberlyst-15 for one-pot synthesis of furfural from xylose. Conditions: xylose (0.67 mmol), isomerization catalyst (0.2 g), Amberlyst-15 (0.1 g), *N*,*N*-dimethylformamide (3 mL), 373 K, 3 h, N_2 flow (30 mL min^{-1}), amount of Cr (9 wt%).

supports seemed to possess no active sites effective for xylose conversion. However, Cr supported SiO_2, CeO_2, TiO_2(rutile), and TiO_2(anatase) showed better activities than bare supports. These results suggest that Cr^{3+} species itself can convert xylose as Lewis acid sites. Efficient production of furfural was observed with combined use of Amberlyst-15 and Lewis acidic AlOOH, γ-Al_2O_3, or Brønsted basic Mg-Al LDH. Increasing furfural production amounts by Cr^{3+} support was also observed for those active supports.

Román-Leshkov *et al.* have reported that aldoses are isomerized into ketoses, which can be dehydrated into furfural by Brønsted acid site, *via* intermolecular MPV reduction over Lewis acid site.[52] We therefore expect that Lewis acidity directly affects the furfural production amount. Figure 4(A) portrays correlation between Lewis acidity of various Cr^{3+} supported catalysts as furfuryl alcohol yield in the MPV reduction and furfural yield in one-pot dehydration of xylose by combined use of Amberlyst-15 and various Cr^{3+} supported catalysts. Actually, good linearity was found: R^2 = 0.99. Nevertheless, Cr/Mg-Al LDH alone did not fit this trend. It showed high activity to furfural synthesis in spite of its Lewis acidity. Given simply, this was apparently true because of the Brønsted basicity of Mg-Al LDH. In the case of Cr/Mg-Al LDH, the furfural yield is affected not only by Lewis acidity originated Cr^{3+} species but also by Brønsted basicity originated Mg-Al LDH. Therefore, if this specifically high activity occurred because of the simple coexistence of Brønsted base site of Mg-Al LDH, these plots show linearity when these were modified to differences of catalytic activities between Cr/Support and Support itself. However, even when modifying these plots to differences of yields between Cr/Support and the support itself ([Yield over Cr/Support] – [Yield over Support]), the Cr/Mg-Al LDH system showed a significantly higher furfural yield than that suggested by the tendency shown by other Cr^{3+} supported catalysts (Figure 4(B)). This result shows clearly that combination of Lewis acidic Cr^{3+} oxide and Brønsted basic Mg-Al LDH exhibited a significant effect on xylose isomerization. Our previous reports confirmed that the combined use of Amberlyst-15 and physical mixture of γ-Al_2O_3 + Mg-Al LDH, a pair of a typical Lewis acid and Brønsted base, showed lower activity to one-pot synthesis of furfural from xylose than the combined use of Amberlyst-15 and Cr/Mg-Al LDH.[11] Moreover, the combined use of Amberlyst-15 and Ni^{2+}-modified Al_2O_3, which possess close boundaries between Lewis acid γ-Al_2O_3 and Brønsted base fine Ni-Al LDH, facilitated the synthesis of furfural from xylose more efficiently than Amberlyst-15 and a physical mixture of γ-Al_2O_3 and Ni-Al LDH.[54] Therefore, we suggest that the close boundaries between Cr^{3+} oxide and Mg-Al LDH acted as bi-functional Lewis acid – Brønsted base sites (Figure 5(A)), facilitating aldose–ketose isomerization from xylose into ketopentoses.

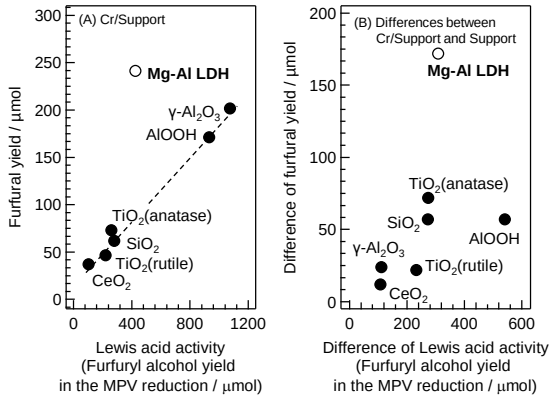

Figure 4. Correlations between catalytic activity for MPV reduction and furfural synthesis over (A) Cr/Supports, and (b) differences of yield between Cr/Support and the support itself ([Yield over Cr/Support](μmol) – [Yield over Support](μmol)). Amount of Cr (9 wt%).

Reaction mechanism. The reaction mechanism for the aldose–ketose isomerization of xylose into xylulose is discussed. Some reports describe two reaction paths from aldose to ketose: a hydride shift mechanism *via* intermolecular MPV reduction catalyzed by Lewis acid such as Sn-Beta,[52] $CrCl_2$ or $CrCl_3$,[50, 61]; and a proton shift mechanism *via* Lobry de Bruyn-Alberda van Ekenstein transformation catalyzed by a base site.[52, 62-63] The rate determining step in both reaction paths is considered to be a hydride/proton shift reaction of deprot-O2-open-aldose (an activated ring opening aldose formed by deprotonation at O2H)[61] or 1,2-endiol(enolate) intermediate[63] (Figures 5(B) & 5(C)). Pidko *et al.* demonstrated that

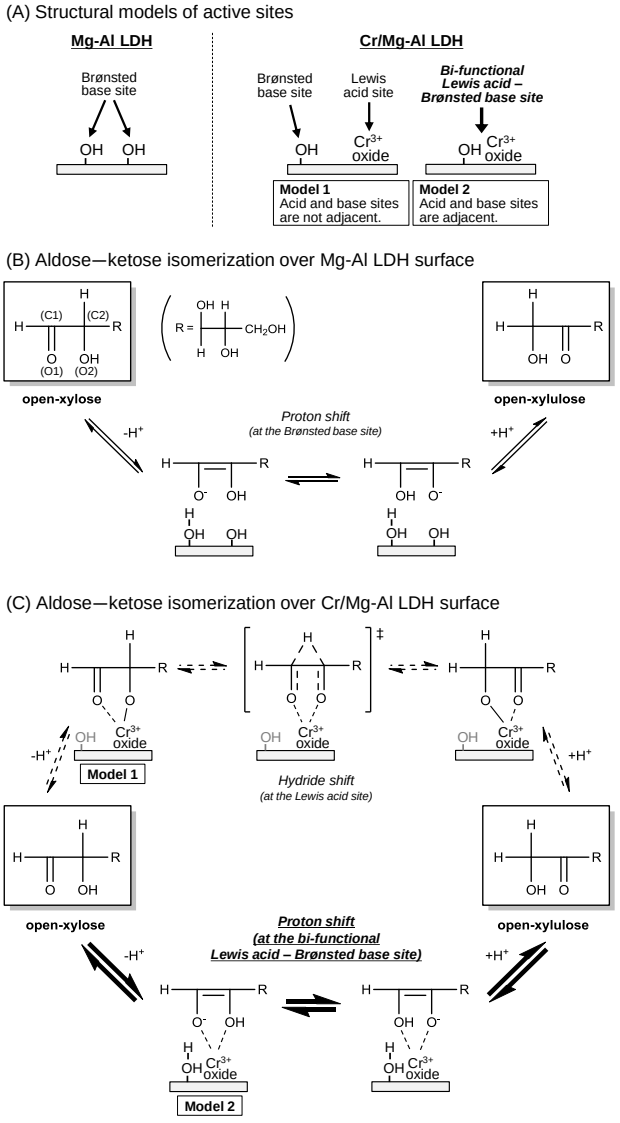

Figure 5. (A) Structural models of active sites on Mg-Al LDH and Cr/Mg-Al LDH surfaces, and the proposed reaction mechanism for aldose–ketose isomerization over (B) Mg-Al LDH and (C) Cr/Mg-Al LDH.

glucose (aldohexose) isomerization toward fructose (ketohexose) was facilitated using Lewis acidic $CrCl_2$ in dialkylimidazolium chloride ionic liquids. They have also described the role of Cr^{2+} ion based on DFT-computed reaction energy diagrams. Two Cr^{2+} ions make coordination with activated sugar intermediate. In the resulting deprot-O2-open-glucose···×2Cr complex, the carbonyl O1 moiety bridges two Cr ions with one of Cr^{2+} additionally coordinating to the anionic O2 group. Interaction with the two metal cations substantially stabilized the anionic reaction intermediates involved in the H shift reaction.[61] Ekeberg *et al.* reported that the reaction rate of the Lobry de Bruyn-Alberda van Ekenstein transformation of aldose to ketose in boiling pyridine was increased strongly by the addition of aluminum oxide. In this catalytic system, the base pyridine is regarded as the main active site. The catalytic effect of aluminum oxide is presumably attributable to adsorption on the surface and stabilization of the enediol intermediate produced by the rate-determining proton shift step by base, thereby lowering the energy of the transition state.[63]

Based on these reports, we propose the possible aldose–ketose isomerization mechanism over bare Mg-Al LDH and Cr/Mg-Al LDH as shown in Figure 5. In the case of bare Mg-Al LDH, at first the deprotonation of C2H of the open-xylose, an α-proton of carbonyl, by the basic site generates unstable 1,2-endiol(enolate) intermediate. Then successive rate-determining proton shifts from O2 to O1 and protonation of C1H occur to form open-xylulose (Figure 5(B)). However, in the case of Cr/Mg-Al LDH (Figure 5(C)), Lewis acid Cr^{3+} oxides make coordination with O1 and O2(H) of open-xylose, which increases positive charges on C2H and O2H. At the close boundaries between Cr^{3+} oxide and Mg-Al LDH, the bi-functional Lewis acid – Brønsted basic sites, the C2H is deprotonated by Brønsted base sites. Also, the isomerization reaction proceeds in the same proton shift process as bare Mg-Al LDH. Unstable 1,2-endiol(enolate) intermediate is expected to be generated as the coordination complex with Lewis acid Cr^{3+} oxide in this case. Therefore, the transition state energy is decreased and the reaction rate is increased compared to that proceeding over bare Mg-Al LDH. Moreover, even at Lewis acid Cr^{3+} oxide, which is not adjacent to the base site, O2H of coordination complex of open-xylose with Cr^{3+} oxide can be deprotonated. A successive intermolecular MPV hydride shift reaction would occur to form open ketopentoses in the same process as Lewis acidic Cr supported SiO_2, CeO_2, TiO_2(rutile), TiO_2(anatase), AlOOH, or γ-Al_2O_3.

Accordingly, we propose that the bi-functional Lewis acid – Brønsted basic sites constructed on Cr/Mg-Al LDH enhance the proton shift mechanism as a main reaction path, and propose that the parts of isolated Cr^{3+} oxides on Cr/Mg-Al LDH proceed by the hydride shift mechanism as a side reaction path. Therefore, such complementary isomerization paths of xylose into ketopentoses over Cr/Mg-Al LDH serve successively higher activity rather than bare Mg-Al LDH and other Cr supported catalysts, leading to high yield for the one-pot formation of furfural.

Effects of the loading amount in Cr supported Mg-Al LDHs. Results show that the loading amount of Cr^{3+} oxide also strongly affects catalytic activity and structural properties in Cr/Mg-Al LDH (*vide infra*). First, the crystal properties of Mg-Al LDH support, electronic states, and local structural properties of Cr species on Cr/Mg-Al LDHs with various Cr loading amounts were evaluated using XRD, XPS, XAS, DTA, and ESR measurements. No significant change of diffraction patterns in accordance with the Cr amount was found using XRD measurements (Figure S4). Even for 15wt%Cr/Mg-Al LDH, only LDH originated XRD patterns were observed. No other Cr^{3+} originated structure such as crystalline α-Cr_2O_3 was detected. Lattice parameters *a* and *c*, which are calculated respectively from (003) and (110) plane diffraction peaks, were almost comparable irrespective of Cr loading amounts, as shown in Figure S5. The XPS analysis of all Cr/Mg-Al LDHs exhibited a Cr $2p_{2/3}$ peak at around 576.5 eV corresponding to the Cr^{3+} oxide. The normalized XPS spectra were almost identical at all Cr loading amounts (Figure S6). Figure 6 shows Cr *K*-edge XANES spectra of various Cr/Mg-Al LDHs and Mg-Cr LDH, amorphous $Cr(OH)_3{\cdot}nH_2O$, and crystalline α-Cr_2O_3 as Cr^{3+} references. All XANES of Cr/Mg-Al LDHs showed Cr^{3+}-originated main peak and some small pre-edge peaks at around 5988–5994 eV. These pre-edges are attributed to distorted octahedral Cr^{3+} of 1s to 3d(2g), 1s to3d(e2g),[64-65] and metal–metal transitions.[65-66] Overall XANES shapes of Cr/Mg-Al LDHs appeared to be intermediate of Mg-Cr LDH and $Cr(OH)_3{\cdot}nH_2O$. It is interesting that only 1wt%Cr/Mg-Al LDH showed a sharp XANES spectral shape in comparison to others, which is more similar to Mg-Cr LDH than $Cr(OH)_3{\cdot}nH_2O$. The 3–15wt%Cr/Mg-Al LDHs shape resembled amorphous $Cr(OH)_3{\cdot}nH_2O$ more than it resembled Mg-Cr LDH.

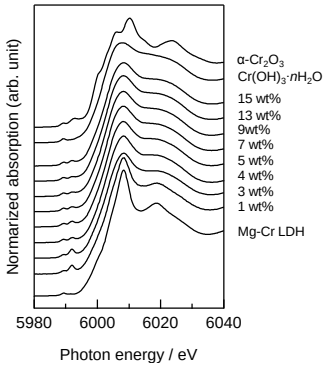

Figure 6. Cr *K*-edge XANES of reference samples and Cr/Mg-Al LDHs with various Cr loadings.

A similar trend was observed from Cr *K*-edge k^3-weighted extended X-ray absorption fine structure (EXAFS) spectra of Cr/Mg-Al LDHs with various Cr loadings (Figure 7(A)). For 3–15 wt%, although the EXAFS spectra were only slightly varied in the region above 9 $Å^{-1}$, the overall shapes in oscillation were almost identical. Whereas, the articulate difference in 1 wt% was observed in the oscillation region around 5.5 and 8.5 $Å^{-1}$. Moreover, the respective shapes in oscillation of 3–15 wt% and 1 wt% were similar to those of amorphous $Cr(OH)_3{\cdot}nH_2O$ and Mg-Cr LDH. These results suggest that the Cr^{3+} species were trapped at first by peripheral defect sites of two-dimensional Mg-Al hydroxide sheets to form substituted Mg-Cr LDH like structure. Subsequently, they adsorbed onto LDH flat plane surface to generate a Cr^{3+} oxide monomer or cluster that has $Cr(OH)_3{\cdot}nH_2O$-like amorphous structure. The diffuse reflectance UV-visible (DR UV-vis) spectra of bulk Cr_2O_3, $Cr(OH)_3{\cdot}nH_2O$, $CrCl_3{\cdot}6H_2O$, Mg-Cr LDH and Cr/Mg-Al LDH are presented in Figure S7. Clearly, the coordination environment of Cr^{3+} oxide on Mg-Al LDH is completely different with bulk Cr_2O_3, $Cr(OH)_3{\cdot}nH_2O$, $CrCl_3{\cdot}6H_2O$, so that Cr^{3+} oxides dispersed on Mg-Al LDH surface might form a monomer or cluster rather than the bulk structure of such a type. This point can be clarified by the radial structure function (RSF; Figure 7(B)). The RSFs (the phase shift was not corrected) of Cr/Mg-Al LDHs produced three peaks at 1.6, 2.5, and 2.8 Å. The first and second peaks were assigned respectively as first coordinated Cr-O and second coordinated Cr-(O)-Cr with 1.98 and 3.00 Å.[65] The third

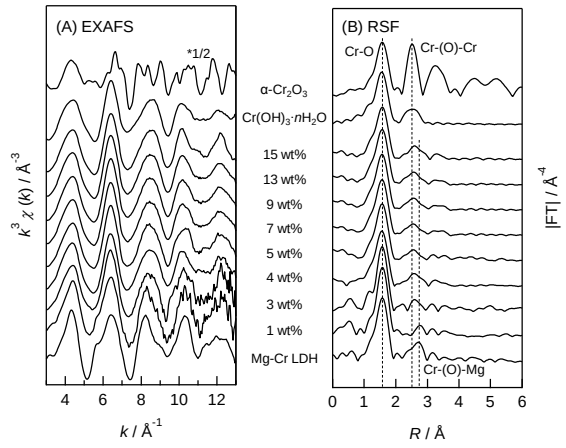

Figure 7. (A) Cr *K*-edge k^3-weighted EXAFS and (b) RSF of reference samples and Cr/Mg-Al LDH with various Cr loadings.

peak is expected to correspond to Cr-(O)-Mg by reference to RSF of Mg-Cr LDH with 3.07 Å.

In the case of 1 wt%, the RSF showed two peaks corresponding to Cr-O and Cr-(O)-Mg. No Cr-(O)-Cr bond was observed. Above 3 wt%, the RSFs peak top at 2.5–2.8 Å, shifted from 2.8 Å (Cr-(O)-Mg) to 2.5 Å (Cr-(O)-Cr) (Figure S8(A)). Then the amplitudes were little increased concomitantly with increasing Cr loading amount (Figure S8(B)). Curve-fitting analysis showed that the coordination numbers of Cr-(O)-Cr were about 1.2 (5 wt%) – 1.4 (15 wt%), indicating that Cr^{3+} oxide mainly formed a dimer or trimer.

Figure 8(A) shows ESR spectra of Cr/Mg-Al LDHs with various Cr loadings recorded at 103 K. Main signals appeared at g = 2.02. Its amplitude increased in accordance with Cr loadings. It is particularly interesting that, in the case of 1 wt%, another signal was visible at g = 4.3 in normalized ESR spectra, as shown in Figure 8(b), whereas this signal was almost reduced in 3 wt%. Reportedly, three ESR responsiveness Cr species exist: (i) the γ-signal with g_{II} = 1.959 and $g_{\perp}$ = 1.978 corresponding to magnetically isolated axially symmetric Cr^{5+} surface species, (ii) the broad line that is visible at g' = 2, which is assigned to magnetically interacting Cr^{3+} ions in Cr_2O_3-like cluster (β-signal), and (iii) the broad line that appeared at g' = 4.3 assigned to magnetically isolated coordinatively unsaturated Cr^{3+} ions (δ-signal).[67] According to a previous report, the two signals appearing in Cr/Mg-Al LDHs at g = 2.02 and g = 4.3 were assigned respectively to Cr^{3+} originated β-signal and δ-signal. These results indicate that a

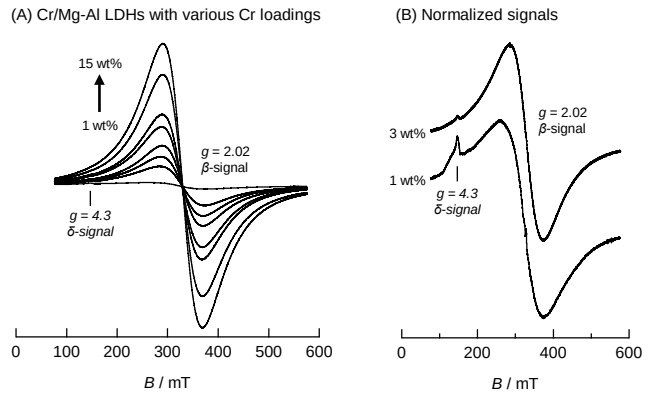

Figure 8. (A) ESR spectra of Cr/Mg-Al LDHs with various Cr loadings and (b) normalized spectra for 1 wt% and 3 wt% at 103 K.

part of Cr^{3+} species on the Mg-Al LDH exist as isolated Cr^{3+} monomer in the case of 1 wt%, and that it forms a Cr_2O_3-like Cr^{3+} cluster (not crystalline) in the cases of above 3 wt%. This result agrees well with XAS results.

A significant change in structural property of Mg-Al LDH support was observed in the DTA curves. Figure 9 shows DTA curves of Cr/Mg-Al LDHs with various Cr loadings. Dehydroxylation of layer hydroxide groups in Mg-Al-CO_3 LDH with Mg/Al = 3 is well known to occur at around 400 °C.[68] As demonstrated in the previous report, bare Mg-Al LDH showed an endothermic peak at 398 °C. The DTA curves of 1–4wt%Cr/Mg-Al LDHs were similar to those of Mg-Al LDH. Above 5 wt%, two shoulder peaks at around 355 °C and 415 °C are apparent. They increased in accordance with Cr loading. Figure S9 shows DTA peaks of various Cr^{3+} references with 15wt%Cr/Mg-Al LDH. Compared to the references, the extra endothermic peak at 355 °C was similar to that of Mg-Cr LDH with Mg/Cr = 5. Because an endothermic peak of Mg-Cr LDH with Mg/Cr = 3 is apparent at 402 °C, the peak at 355 °C is expected to originate from dehydroxylation of unstable Mg excess Mg-Cr composite hydroxide, such as $Mg_2Cr(OH)$. Another peak at 415 °C was only observed in the partially substituted Mg-Al-Cr LDH, indicating that this extra peak is attributed to dehydroxylation of MgAlCr(OH) site. These results suggest that Cr^{3+} species are dispersed mainly onto LDH surface up to 5 wt%. Then excess Cr^{3+} species generate Mg-Cr and/or Mg-Al-Cr LDH like composite structure above 5 wt%. Figure S10 portrays TEM images of bare Mg-Al LDH and Cr/Mg-Al LDH with various Cr loadings. LDH originated layered flat plane was observed in all samples. The morphology of Cr/Mg-Al LDH below 5 wt% was as smooth as that of bare Mg-Al LDH, although it became coarse above 5 wt%. Furthermore, no Cr^{3+} originated articulate particles were observed. Because no change in lattice parameter of Mg-Al LDH support with various Cr loadings was observed, as shown in Figure S5, these results support that Cr^{3+} oxides were covering the LDH carrier as small size clusters up to 5 wt%, thereafter forming amorphous Mg-Cr and/or Mg-Al-Cr LDH-like composite at the surface of the Mg-Al LDH support.

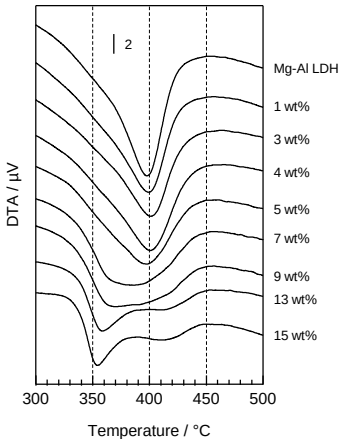

Figure 9. DTA profiles of Cr/Mg-Al LDHs with various Cr loadings.

Based on the intensity of Cr 2p, Mg 2p and Al 2p XPS, the surface Cr/(Mg+Al) ratio was calculated as shown in Figure S11. The surface Cr/(Mg+Al) ratio was linearly increased in accordance with Cr loading up to 5 wt%. Thereafter, its increase became gradual. This result showed clearly that 5 wt% is a criterion that differentiates the character of Cr^{3+} species in Cr/Mg-Al LDH: most Cr^{3+}species are apparently supported on the Mg-Al LDH surface in the case of below 5 wt%, although a part of it substitutes brucite layer of LDH

or forms Mg-Cr and/or Mg-Al-Cr composite. The specific surface areas (S_{BET}) of Cr/Mg-Al LDHs with various Cr loadings are presented in Table S2 and are shown in Figure S12. The Cr theoretical content, Cr content obtained by ICP-AES, surface area g(Mg-Al LDH)$^{-1}$ (S_0) calculated from S_{BET}, occupied area by Cr_2O_3 ($S_{occupied}$) calculated from Cr content, and theoretical coverage (ϑ) by Cr_2O_3 on Mg-Al LDH are listed in Table S2. To calculate S_0, $S_{occupied}$ and ϑ, we applied three assumptions: (i) all Cr^{3+} species exist as Cr_2O_3 octahedral, (ii) all Cr_2O_3 units have the same cross section, and (iii) the value of cross section is 0.16 nm^2 per Cr_2O_3. In the range of 0–5 wt%, S_{BET} was increased gradually from 44.5 to 83.6 m^2 g^{-1}. Thereafter, it increased rapidly and reached 238 m^2 g^{-1} (15 wt%). It is particularly interesting that S_0 showed the same trend with S_{BET}, indicating that the surface area of the LDH carrier itself is varied with Cr loading amount. Cr/Mg-Al LDHs were prepared in acidic $CrCl_3 \cdot 6H_2O$ aqueous solution with pH = 3–3.5. Therefore, this change of S_0 with Cr loadings is expected to be attributable to the dissolution and reprecipitation of LDH carrier with Cr^{3+} ion. It is noteworthy that simple treatment of Mg-Al LDH in aqueous hydrochloric solution of pH 3, the same pH with $CrCl_3 \cdot 6H_2O$ aqueous solution for preparation of 15 wt%Cr/Mg-Al LDH, did not strongly affect the increase of S_{BET} (52.4 m^2 g^{-1}). Because this change becomes prominent above 5 wt%, the point at which Mg-Al-Cr LDH composite begins to be generated, the amorphous Mg-Al-Cr composite might possess high surface area. Their generation might contribute to the improvement of S_{BET} and S_0. For 4–5 wt%, S_0 and $S_{occupied}$ were calculated respectively as 78.1–90.1 m^2 g^{-1} and 75.6–96.4 m^2 g(Mg-Al LDH)$^{-1}$. The theoretical ϑ at 4–5 wt% calculated from those values were 96.8–107%, indicating that most of the LDH surface was covered with a monolayer of Cr^{3+} oxide at 4–5 wt%.

Next, we investigated the effects of Cr loading amounts on catalytic activities. Figure 10(A) shows the correlation of furfural yield and Cr loading amounts in the one-pot synthesis of furfural from xylose using Amberlyst-15 and Cr/Mg-Al LDHs with various Cr loadings. Among the 0–15wt%Cr/Mg-Al LDH, 5wt%Cr/Mg-Al LDH catalyst showed the highest furfural yield (40%). Additionally, when those catalytic systems were applied to one-pot synthesis of FMM from xylose *via* successive Knoevenagel condensation of generated furfural with malononitrile, again 5wt%Cr/Mg-Al LDH showed the highest activity (49% yield with 94% selectivity, Figure 10(B)). Selectivity for FMM varied in accordance with the Cr amount: it decreased immediately for 0–5 wt% Cr loadings; thereafter the reduction rate became gradual. Our previous report described that successive Knoevenagel condensation is catalyzed mainly by Brønsted base sites of Mg-Al LDH.[11] Therefore, this change in selectivity up to 5 wt% might occur because of the decrement of Mg-Al LDH-originated Brønsted base sites by Cr loading. Furthermore, above 5 wt%, generation of Mg-Cr and/or Mg-Al-Cr LDH-like composite might act as weak Brønsted base site to suppress the decrease of the reaction rate for Knoevenagel condensation. The absence of leaching of Cr after the reaction was confirmed by ICP-AES analysis, but the catalytic activity was reduced in the reuse experiments because of the adsorption of intermediate and other by-products onto the Cr/Mg-Al LDH.[11]

To elucidate the correlation between activities for xylose transformation and Lewis acidity in Cr/Mg-Al LDH system, we attempted to evaluate the activity derived from Lewis acidic sites on Cr/Mg-Al LDHs with various Cr loadings using the MPV reduction. Figure 11(A) shows that the simple increase in initial rate per weight of Cr/Mg-Al LDH by the increase in Cr loading amount was observed. Furthermore, when the initial rates for the MPV reduction were

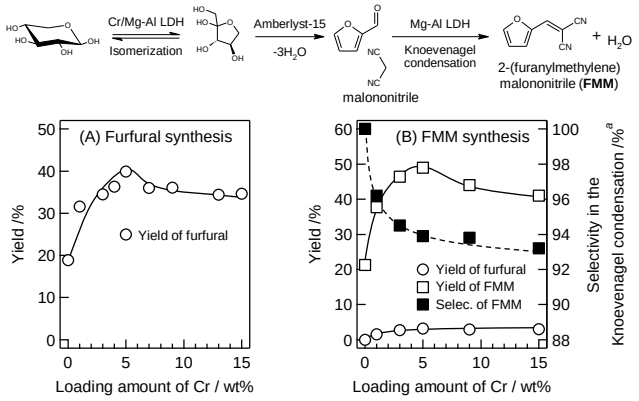

Figure 10. Activities of combined use of Amberlyst-15 and Cr/Mg-Al LDHs with various Cr loadings for one-pot transformation of xylose into (A) furfural and (b) FMM. Conditions: (A) xylose (0.67 mmol), isomerization catalyst (0.2 g), Amberlyst-15 (0.1 g), *N*,*N*-dimethylformamide (3 mL), 373 K, 3 h, N_2 flow (30 mL min^{-1}). (B) after (a), the reaction mixture was cooled to room temperature without stirring. Then 0.8 mmol of malononitrile was added, and the reaction was restarted. 1 h, N_2 flow (30 mL min^{-1}). ^{a}Selectivity: $Yield_{FMM}/(Yield_{furfural} + Yield_{FMM}) \times 10^2$.

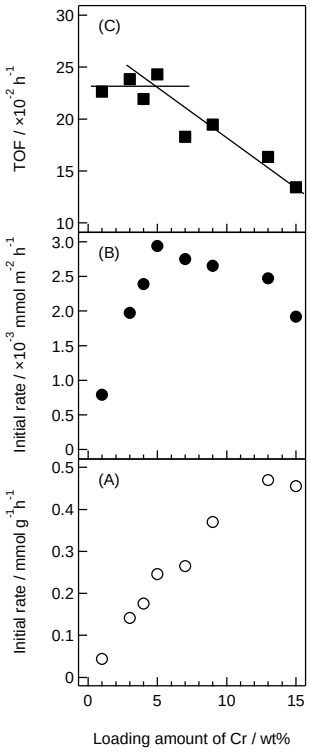

Figure 11. Lewis acidic activities of Cr/Mg-Al LDHs with various Cr loadings for the MPV reduction as (A) initial rate per unit weight of Cr/Mg-Al LDH, (B) initial rate per unit surface area of Cr/Mg-Al LDH and (c) apparent TOF of Cr species. Conditions: furfural (1.3 mmol), 2-propanol (83 mmol), catalyst (0.1 g), 355 K, 1 h, amount of Cr (9 wt%). TOF: Initial rate (mmol g^{-1} h^{-1}) / amount of Cr (mmol g^{-1}).

divided by specific surface area S_{BET}, a different trend was observed as shown in Figure 11(B): the initial rate per unit surface area of Cr/Mg-Al LDH increased linearly to 5 wt%. Then it decreased gradually. This change presumably occurs because of generation of

the amorphous Mg-Cr and/or Mg-Al-Cr LDH-like composite (*vide supra*). Moreover, when the initial rates for the MPV reduction were divided by the total Cr loading amount to calculate the apparent turnover frequency (TOF), the 5 wt% was found as a criterion again, the Lewis acidity of Cr^{3+} species in Cr/Mg-Al LDH changes. The TOFs of Cr species were almost equal for <5 wt%, but these values were decreased above 5 wt%. These facts indicate that Cr^{3+} oxide retained its Lewis acidity for <5 wt%, although a part of Cr^{3+} species which are forming Mg-Cr and/or Mg-Al-Cr LDH like composite cannot act efficiently as a Lewis acid site for >5 wt%.

According to these results for characterizations and catalytic activities for Cr/Mg-Al LDHs with various Cr loadings, the 5 wt% Cr loading was found as the key point for the appearance of some characteristics: (1) Mg-Cr and/or Mg-Al-Cr LDH-like composite begins to be generated. (2) The LDH carrier is almost covered with a monolayer of Cr^{3+} oxide. (3) The activity for furfural synthesis is maximized. (4) The Lewis acid activity of Cr^{3+} species begins to decline. Kitano *et al.* reported that a Nb_2O_5, Ta_2O_5, MoO_3 or WO_3 monolayer or small cluster was generated on the Al_2O_3 carrier surface after calcination of Nb_2O_5, Ta_2O_5, MoO_3 or WO_3/Al_2O_3 at 1073–1223 K. These exhibited high thermal stable Brønsted acidity at the boundary of supported metal oxide monolayer domains.[69-72] For Nb_2O_5, Ta_2O_5 and MoO_3/Al_2O_3, when the supported metal oxide loading exceeded the amount necessary to form a two-dimensional metal oxide overlayer, inert Al-containing compounds such as $AlNbO_4$, $AlTaO_4$, and $Al_2Mo_3O_{12}$ were formed and were deposited on some Brønsted acid sites, thereby lowering the catalytic activity. Based on these reports, we infer the effect of Cr loading amount on the physical property and catalytic activity of Cr/Mg-Al LDH as follows. First, a part of a Cr^{3+} oxide monomer is trapped by peripheral defect sites of two-dimensional Mg-Al hydroxide sheets. Others are supported onto Mg-Al LDH surface in the case of the low Cr loading amount (>1 wt%). Second, the supported Cr^{3+} oxide forms a dimer or trimer cluster. It covers the Mg-Al LDH carrier surface up to 5 wt%. Because these Cr^{3+} monomers, dimers, and trimers act as Lewis acid sites, the cross boundaries between small Cr^{3+} clusters and the LDH surface form bi-functional Lewis acid – Brønsted base sites that are highly active sites for xylose isomerization. Third, when the Cr^{3+} loading exceeds the amount necessary to cover the Mg-Al LDH carrier (>5 wt%), excess Cr^{3+} species form non-Lewis acidic Mg-Cr and/or Mg-Al-Cr LDH-like composite and are deposit on some active Lewis acid – Brønsted base sites, thereby lowering the activity.

From these results, we infer that the 5 wt%Cr/Mg-Al LDH possesses the most effective interaction between Lewis acidic Cr^{3+} oxide and Mg-Al LDH basic site, giving superior catalytic activity for xylose conversion.

Homogeneous and heterogeneous catalytic dehydration of xylose to furfural at 373 K have been reported by some research groups. Binder *et al.* have demonstrated that 56% yield of furfural was observed by using 6 mol% $CrCl_2$ with LiBr in *N*,*N*-dimethylacetamide for 4 h.[50] Suzuki *et al.* have reported that heterogeneous SO_4^{2-}/SnO_2 catalyst afforded 26.6% yield of furfural for 48 h.[51] This reaction condition is more preferable because heterogeneous solid catalysts can be easily removed from solution after catalytic reaction, and they used only 50 mg catalyst against to 1 mmol of xylose. However, this system has a lower furfural yield relative to take a long reaction time. In this research, the combined use of 5 wt%Cr/Mg-Al LDH and Amberlyst-15 successfully converted xylose into furfural with 59% yield at 18 h reaction time (Figure S13). Although our catalytic system requires higher weight ratio for catalyst : xylose than Suzuki's report, this yield was the highest value among all those reported for previous studies conducted at 373 K.[11, 18, 50-51, 54] Additionally, this catalytic system showed high activity to direct synthesis of FMM from xylose *via* the successive Knoevenagel condensation of generated furfural with malononitrile. It performed 59% yield of FMM at 18 h of furfural synthesis from xylose and 5 h of successive Knoevenagel condensation in a one-pot manner.

Conclusions

One-pot synthesis of furfural from xylose was done successfully by the combined use of Brønsted acid Amberlyst-15 and bi-functional Lewis acid – Brønsted base Cr/Mg-Al LDH. The bi-functional Lewis acid – Brønsted base sites of Cr/Mg-Al LDH are expected to be generated at the cross boundaries between Lewis acidic Cr^{3+} oxide and Brønsted basic LDH surface. Xylose isomerization, the rate-determining step of the one-pot reaction, was promoted efficiently at the bi-functional Lewis acid – Brønsted base sites of Cr/Mg-Al LDH by proceeding proton shift reaction of the coordination complex of xylose with Lewis acid Cr^{3+} oxide, leading to higher furfural yield than basic bare Mg-Al LDH, substituted Mg-Cr LDH, and Lewis acidic other Cr supported catalysts. The surface structure and catalytic activities of Cr/Mg-Al LDH were varied with Cr loadings. The highest furfural and FMM yields were obtained by combined use of 5 wt%Cr/Mg-Al LDH and Amberlyst-15 with 59% yield at 373 K. XRD, XPS, XAS, ESR, DTA, N_2 adsorption measurement and MPV reduction revealed that (1) the monomer of Lewis acidic Cr^{3+} oxide is immobilized on the Mg-Al LDH surface below 1 wt%, (2) up to 5 wt%, Cr^{3+} species form Lewis acidic Cr^{3+} oxide dimer or trimer with covering Mg-Al LDH to generate highly active bi-functional Lewis acid – Brønsted base sites, (3) above 5 wt%, excess Cr^{3+} species form inert Mg-Cr and/or Mg-Al-Cr LDH-like composites and are deposited on some active bi-functional Lewis acid – Brønsted base sites, leading to lower activity. Therefore, we presume that the 5 wt%Cr/Mg-Al LDH surface that comprises LDH carrier and covering layer of Cr^{3+} oxide possesses the most effective interaction between Lewis acidic Cr^{3+} oxide and basic Mg-Al LDH surface to generate abundant bi-functional Lewis acid – Brønsted base sites, leading to the best catalytic activity. In the investigation of correlation between catalytic activity and structural properties of Cr/Mg-Al LDH with various Cr loadings, we elucidated the local structure and optimum preparation method of bi-functional Lewis acid – Brønsted base sites over LDH-based catalysts to propose a new technique to control acid–base bi-functional solid surfaces.

Acknowledgements

This work was supported by a Grant-in-Aid from Japan Society for the Promotion of Science (JSPS) Fellows (No. 15J10050). The authors are indebted to Prof. Yusuke Yoshinaga (Department of Molecular Chemistry, Tokyo Gakugei University) for his great help with ESR experiments. Preliminary XAS experiments were

conducted at BL01B1 in SPring-8 (Proposal Nos. 2015A1389 and 2014B1472).

References

1 K. Kaneda, T. Yamashita, T. Matsushita, and K Ebitani, *J. Org. Chem.*, 1998, **63**, 1750.
2 N. Kakiuchi, Y. Maeda, T. Nishimura, and S. Uemura, *J. Org. Chem.,* 2001, **66**, 6620.
3 K. Motokura, D. Nishimura, K. Mori, T. Mizugaki, K. Ebitani, and K. Kaneda, *J. Am. Chem. Soc.,* 2004, **126**, 5662.
4 T. Mitsudome, Y. Mikami, H. Funai, T. Mizugaki, K. Jitsukawa, and K. Kaneda, *Angew. Chem. Int. Ed.,* 2008, **47**, 138.
5 W. Fang, Q. Zhang, J. Chen, W. Deng, and Y. Wang, *Chem. Commun.,* 2010, **46**, 1547.
6 A. Tsuji, K. T. V. Rao, S. Nishimura, A. Takagaki, and K. Ebitani, *ChemSusChem* 2011, **4**, 542.
7 S. Nishimura, A. Takagaki, and K. Ebitani, *Green Chem.,* 2013, **15**, 2026.
8 M. L. Kantam, B. M. Choudary, C. V. Reddy, K. K. Rao, M. L. Kantam, B. M. Choudary, K. K. Rao, and F. Figueras, *Chem. Commun.,* 1998, 1033.
9 M. Climent, *J. Catal.,* 2004, **225**, 316.
10 E. Angelescu, O. D. Pavel, R. Bîrjega, R. Zăvoianu, G. Costentin, and M. Che, *Appl. Catal. A*, 2006, **308**, 13.
11 M. Shirotori, S. Nishimura, and K. Ebitani, *Catal. Sci. Technol.,* 2014, **4**, 971.
12 K. Yamaguchi, K. Mori, T. Mizugaki, K. Ebitani, and K. Kaneda, *J. Org. Chem.,* 2000, **65**, 6897.
13 T. Honma, M. Nakajo, T. Mizugaki, K. Ebitani, and K. Kaneda, *Tetrahedron Lett.,* 2002, **43**, 6229.
14 E. Li, Z. P. Xu, and V. Rudolph, *Appl. Catal., B* 2009, **88**, 42.
15 Z. An, W. Zhang, H. Shi, and J. He, *J. Catal.,* 2006, **241**, 319.
16 H. C. Greenwell, P. J. Holliman, W. Jones, and B. V. Velasco, *Catal. Today*, 2006, **114**, 397.
17 M. Ohara, A. Takagaki, S. Nishimura, and K. Ebitani, *Appl. Catal. A*, 2010**, 383**, 149.
18 A. Takagaki, M. Ohara, S. Nishimura, and K. Ebitani, *Chem. Lett.,* 2010, **39**, 838.
19 A. Takagaki, M. Takahashi, S. Nishimura, and K. Ebitani, *ACS Catal.,* 2011, **1**, 1562.
20 G. W. Huber, J. N. Chheda, C. J. Barrett, and J. A. Dumesic, *Science*, 2005, **308**, 1446.
21 R. Karinen, K. Vilonen, and M. Niemelä, *ChemSusChem*, 2011, **4**, 1002.
22 P. Gallezot, *Chem. Soc. Rev.,* 2012, **41**, 1538.
23 C. O. Tuck, E. Pérez, I. T. Horváth, R. A. Sheldon, and M. Poliakoff, *Science*, 2012, **337**, 695.
24 G. W. Huber, S. Iborra, and A. Corma, *Chem. Rev.,* 2006, **106**, 4044.
25 J. N. Chheda, G. W. Huber, and J. A. Dumesic, *Angew. Chem. Int. Ed.,* 2007, **46**, 7164.
26 C. H. Zhou, X. Xia, C. X. Lin, D. S. Tong, and J. Beltramini, *Chem. Soc. Rev.,* 2011, **40**, 5588.
27 H. Kobayashi, and A. Fukuoka, *Green. Chem.,* 2013, **15**, 1740.
28 J. S. Luterbacher, D. M. Alonso, and J. A. Dumesic, *Green Chem.,* 2014, **16**, 4816.
29 H. Kobayashi, M. Yabushita, T. Komanoya, K. Hara, I. Fujita, and A. Fukuoka, *ACS Catal.,* 2013, **3**, 581.
30 P.-W. Chung, A. Charmot, O. A. Olatunji-Ojo, K. A. Durkin, and A. Katz, *ACS Catal.,* 2014, **4**, 302.
31 P.-W. Chung, M. Yabushita, A. T. To, Y. Bae, J. Jankolovits, H. Kobayashi, A. Fukuoka, and A. Katz, *ACS Catal.,* 2015, **5**, 6422.
32 A. T. To, P.-W. Chung, and A. Katz, *Angew. Chem. Int. Ed.,* 2015, **54**, 11050.
33 S. Suganuma, K. Nakajima, M. Kitano, D. Yamaguchi, H. Kato, S. Hayashi, and M. Hara, *J. Am. Chem. Soc.,* 2008, **130**, 12787.
34 X. Zhao, J. Wang, C. Chen, Y. Huang, A. Wang, T. Zhang, *Chem. Commun.,* 2014, **50**, 3439.
35 P. Dornath, H. J. Cho, A. Paulsen, P. Dauenhauer, and W. Fan, *Green Chem.,* 2015, **17**, 769.
36 H. Kobayashi, H. Kaiki, A. Shrotri, K. Techikawara, and A. Fukuoka, *Chem. Sci.,* 2016, **7**, 692.
37 H. Choudhary, S. Nishimura, and K. Ebitani, *Chem. Lett.,* 2012, **41**, 409.
38 B. Danon, G. Marcotullio, W. de Jong, *Green Chem.,* 2014, **16**, 39.
39 A. S. Dias, S. Lima, M. Pillinger, and A. A. Valente, *Catal. Lett.,* 2007, **114**, 151.
40 A. S. Dias, S. Lima, P. Brandão, M. Pillinger, J. Rocha, and A. A. Valente, *Catal. Lett.,* 2006, **108**, 179.
41 G. H. Jeong, E. G. Kim, S. B. Kim, E. D. Park, and S. W. Kim, *Microporous and Mesoporous Mater.,* 2011, **144**, 134.
42 I. Agirrezabal-Telleria, J. Requies, M. B. Güemez, and P. L. Arias, *Appl. Catal. B*, 2014, **145**, 34.
43 A. S. Dias, M. Pillinger, and A. A. Valente, *Appl. Catal. A*, 2005, **285**, 126.
44 S. Lima, M. Pillinger, and A. Valente, *Catal. Commun.,* 2008, **9**, 2144.
45 R. O'Neill, M. N. Ahmad, L. Vanoye, and F. Aiouache, *Ind. Eng. Chem. Res.,* 2009, **48**, 4300.
46 S. Lima, A. Fernandes, M. M. Antunes, M. Pillinger, F. Ribeiro, and A. A. Valente, *Catal. Lett.,* 2010, **135**, 41.
47 R. Weingarten, J. Cho, J. Wm. Curtis Conner, and G. W. Huber, *Green Chem.,* 2010, **12**, 1423.
48 M. J. Climent, A. Corma, and S. Iborra, *Green Chem.,* 2011, **13**, 520.
49 V. Choudhary, S. I. Sandler, and D. G. Vlachos, *ACS Catal.,* 2012, **2**, 2022.
50 J. B. Binder, J. J. Blank, A. V. Cefali, and R. T. Raines, *ChemSusChem*, 2010, **3**, 1268.
51 T. Suzuki, T. Yokoi, R. Otomo, J. N. Kondo, and T. Tatsumi, *Appl. Catal. A*, 2011, **408**, 117.
52 Y. Roman-Leshkov, M. Moliner, J. A. Labinger, and M. E. Davis, *Angew. Chem. Int. Ed.,* 2010, **49**, 8954.
53 H. S. Soliman, M. Eid Kh, H. A. Ali, M. A. El-Mansy, and S. M. Atef, *Spectrochim. Acta A Mol. Biomol. Spectrosc.,* 2013, **105**, 545.
54 M. Shirotori, S. Nishimura, and K. Ebitani, *Chem. Lett.,* 2016, **45**, 194.
55 P. Keller, and H.-H. Strehblow, *Corros. Sci.,* 2004, **46**, 1939.
56 M. J. Gilkey, and B. Xu, *ACS Catalysis*, 2016, **6**, 1420.
57 M. A. Aramendía, V. Borau, C. Jiménez, J. M. Marinas, J. R. Ruiz, and F. J. Urbano, *Appl. Catal. A*, 2003, **255**, 301.M.
58 M. A. Aramendía, V. Borau., C. Jiménez, J. M. Marinas, J. R. Ruiz, and F. J. Urbano, *J. Mol. Catal. A*, 2001, **171**, 153.
59 M. A. Aramendia, V. Borau, C. Jimenez, J. M. Marinas, J. R. Ruiz, and F. J. Urbano, *J Colloid. Interface Sci.*, 2001, **238**, 385.
60 H. Hattori, *Appl. Catal. A*, 2001, **222**, 247.
61 E. A. Pidko, V. Degirmenci, and E. J. M. Hensen, *ChemCatChem*, 2012, **4**, 1263.
62 D. Ekeberg, S. Morgenlie, and Y. Stenstrom, *Carbohydr. Res.,* 2005, **340**, 373.
63 D. Ekeberg, S. Morgenlie, and Y. Stenstrom, *Carbohydr. Res.,* 2007, **342**, 1992.
64 S. G. Eeckhout, N. Bolfan-Casanova, C. McCammon, S. Klemme, and E. Amiguet, *Am. Mineral.,* 2007, **92**, 966.
65 N. Papassiopi, F. Pinakidou, M. Katsikini, G. S. Antipas, C. Christou, A. Xenidis, and E. C. Paloura, *Chemosphere*, 2014, **111**, 169.
66 J. Frommer, M. Nachtegaal, I. Czekaj, and R. Kretzschmar, *Am. Mineral.,* 2010, **95**, 1202.
67 Weckhuysen, B. M., *Chem. Commun.,* 2002, 97.
68 J. Zhang, Y. F. Xu, G. Qian, Z. P. Xu, C. Chen, and Q. Liu, *J. Phys. Chem. C*, 2010, **114**, 10768.

69 T. Kitano, S. Okazaki, T. Shishido, K. Teramura, and T. Tanaka, *Catal. Today*, 2012, **192**, 189.
70 T. Kitano, T. Shishido, K. Teramura, and T. Tanaka, *J. Phys. Chem. C*, 2012, **116**, 11615.
71 T. Kitano, S. Okazaki, T. Shishido, K. Teramura, and T. Tanaka, *J. Mol. Catal. A*, 2013, **371**, 21.
72 T. Kitano, T. Hayashi, T. Uesaka, T. Shishido, K. Teramura, and T. Tanaka, *ChemCatChem*, 2014, **6**, 2011.

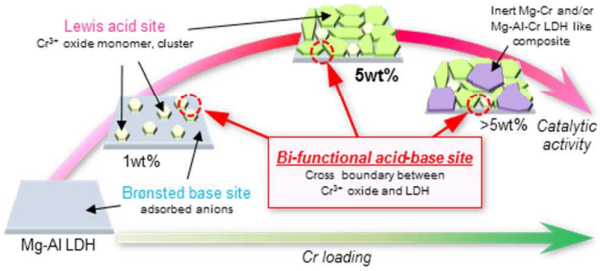

The cross boundary between Cr^{3+} oxide and Mg-Al LDH generate highly active bi-functional acid — base sites for xylose isomerization.